# On the Approximation of Pseudospectra of Nonnormal Operators by Discretization, Part II: the Convection-Diffusion Operator

A. Harrabi

CERFACS Technical Report TR/PA/98/38

**Abstract**

In an earlier report [4], the pseudospectrum of the first derivative operator discretized by spectral and finite difference methods has been analyzed. Here, the same work is carried out for the convection-diffusion operator. The high sensitivity of the pseudospectrum of the operator under several discretization methods is illustrated by numerous examples.

**Key words:** pseudospectra, convection-diffusion operator, Galerkin approximation, collocation approximation, finite-difference method.

## 1 Introduction

In a first part [4], we have studied the 1D first derivative operator $T$. We recall that the spectrum $\sigma(T)$ is empty, its $\epsilon$-pseudospectrum $\sigma_\epsilon(T)$ is a left half-plane. We have discretized $T$ by spectral and finite-difference methods. We have shown that the $\epsilon$-pseudospectrum $\sigma_\epsilon(T_N)$ of the discretized matrices $T_N$ can be a good local approximation in the neighborhood of zero of $\sigma_\epsilon(T)$, but a point $z \in \sigma_\epsilon(T)$ with a large module requires a very large order of discretization $N$ to be in $\sigma_\epsilon(T_N)$. We have shown also that the speed of the convergence of $\sigma_\epsilon(T_N)$ to $\sigma_\epsilon(T)$ depends strongly on the discretization scheme.

In this second part, the same work is performed for the 1D convection-diffusion operator $\mathcal{L}$. We will see that globally the same properties of the $\epsilon$-pseudospectra of the discretized matrices are observed.

We will see also that there is a slight modification of the classification of the discretization schemes in the sense that the discretization scheme that produces the best approximation of the pseudospectrum of the operator is not necessarily the same for the 1D first derivative operator and the 1D convection-diffusion operator.

In the case of the convection-diffusion operator, we classify these discretization schemes in increasing accuracy as follows: $i$) finite difference method in Chebyshev points, $ii$) collocation approximation with the Chebyshev points too, $iii$) finite difference method with the equidistant points, and $iv$) Galerkin approximation with the sine basis. We note that, here, the pseudospectra of the operator $\mathcal{L}$ is not known exactly, but, we have at least two approximations $\sigma_{m\epsilon}(\mathcal{L})$ and $\sigma_{s\epsilon}(\mathcal{L})$ such that $\sigma_{m\epsilon}(\mathcal{L}) \subseteq \sigma_{\epsilon}(\mathcal{L}) \subseteq \sigma_{s\epsilon}(\mathcal{L})$. This gives us an idea of the shape and the width of $\sigma_{\epsilon}(\mathcal{L})$. The classification given here is governed by two features: the first one is how $\sigma_{\epsilon}(A_N)$, where $A_N$ denotes a matrix given by some discretized scheme, extends itself in the region limited by the parabola $\{x = -y^2\}$ which known that $\sigma_{\epsilon}(\mathcal{L})$ approximate a parabolic region in a large part near zero, we show latter, in third section, that globally is not. The second feature is the shape of $\sigma_{\epsilon}(A_N)$, and if these $\epsilon$-pseudospectra approximate a parabola near zero.

In addition to the introduction, this paper includes six sections. The second section is devoted to provide some properties of the convection-diffusion operator $\mathcal{L}$. The third section recalls various equivalent definitions of the pseudospectrum for a closed linear operator in a Hilbert space, characterizes the features of the pseudospectrum of $\mathcal{L}$. The fourth section is devoted to explain how to plot the pseudospectrum of the discretized matrices, and how to plot the two sets $\sigma_{m\epsilon}(\mathcal{L})$ and $\sigma_{s\epsilon}(\mathcal{L})$ which are respectively included in and containing $\sigma_{\epsilon}(\mathcal{L})$. The fifth section is devoted to the discretization of the operator $\mathcal{L}$ by finite difference with either Chebyshev or equidistant points, and to study the spectra and the pseudospectra of the resulting matrices. In the sixth section, the operator $\mathcal{L}$ is discretized by spectral methods: collocation approximation with Chebyshev points, and Galerkin approximation with the sine functions as a basis. The spectra and the pseudospectra of the resulting matrix are again studied and plotted.

## 2 Convection-Diffusion Operator

We define the convection-diffusion operator $\mathcal{L}$ acting in the Hilbert space $L^2[0,\ d]$ for some $d > 0$ by

$$\mathcal{L}u = \nu u'' + cu', \quad u(0) = u(d) = 0, \tag{1}$$

where $\nu,\ c > 0$.

The domain of definition $D(\mathcal{L})$ of $\mathcal{L}$ is the Sobolev space $\mathcal{H}_0^2 = \{u \in \mathcal{C}^1[0,\ d];\ u'' \in L^2[0,\ d]$ and $u(0) = u(d) = 0\}$ where $\mathcal{C}^1[0,\ d]$ is the space of functions that possess a first continuous derivative in the $[0,\ d]$ interval. We notice that $D(\mathcal{L})$ is dense in $L^2[0,\ d]$ ; $\mathcal{L}$ is a closed linear operator on $L^2[0,\ d]$ (see [2, 6]).
Moreover, the spectrum $\sigma(\mathcal{L})$ of $\mathcal{L}$ is a discrete subset of the negative real axis and is equal to $\{\lambda_n\}_{n=1,2,\dots}$ where

$$\lambda_n \quad = \quad -\frac{c^2}{4\nu} - \frac{\pi^2 n^2 \nu}{d^2} \qquad \text{for all } n \in \mathbb{N} \tag{2}$$

with respective associated eigenfunctions

$$\phi_n(x) \quad = \quad e^{\alpha_+^n x} - e^{\alpha_-^n x} \qquad \text{for all } n \in \mathbb{N} \tag{3}$$

where $\alpha_\pm^n = -\frac{c}{2\nu} \pm \frac{1}{2}((c/\nu)^2 + 4\lambda_n/\nu)^{1/2}$ for all $n \in \mathbb{N}$.

Consider $z \in \rho(\mathcal{L})$, and $u,\ f \in L^2[0,\ d]$. Then $(z - \mathcal{L})u = f$ is equivalent to $G_z f = u$ where

$$G_z f(y) \quad = \quad \int_0^d g_z(y,x) f(x)\, dx. \tag{4}$$

The Green operator $G_z$ is the Wiener-Hopf integral operator with kernel

$$g_z(y,x) \quad = \quad \begin{cases} -\frac{1}{k} u_1(y) u_2(x) e^x & \text{if} \quad y \leq x; \\ -\frac{1}{k} u_1(x) u_2(y) e^x & \text{if} \quad y \geq x, \end{cases} \tag{5}$$

where $k = (\alpha_+ - \alpha_-)(e^{-\alpha_- d} - e^{-\alpha_+ d}) = \frac{1}{\nu}(c^2 + 4z\nu)^{\frac{1}{2}} e^{\frac{cd}{2\nu}} (e^{\frac{d}{2\nu}(c^2+4\nu z)^{\frac{1}{2}}} - e^{-\frac{d}{2\nu}(c^2+4\nu z)^{\frac{1}{2}}})$, $\alpha_\pm$ are the two different solutions of the equation $z = \alpha^2 + \alpha$, and

$$u_1(x) = e^{\alpha_+ x} - e^{\alpha_- x}, \qquad u_2(x) = e^{\alpha_+ (x-d)} - e^{\alpha_- (x-d)}.$$

We notice that $u_1(0) = 0$ and $u_2(d) = 0$. The function $g_z(y,x)$ is the Green function associated with the problem $(z - \mathcal{L})u = f$ [2, pp. 90-93].

We now show that $\mathcal{L}$ ***is nonnormal***.

Let us first calculate the adjoint operator $\mathcal{L}'$ of $\mathcal{L}$. Let $v \in D(\mathcal{L})$, and $v \in L^2[0,\, d]$.

$$\begin{aligned}(\mathcal{L}u, v) &= \int_0^d \mathcal{L}u(x)\bar{v}(x)\, dx, \\ &= (u, \nu v'' + cv') + \nu\left(u'(d)\bar{v}(d) - u'(0)\bar{v}(0)\right).\end{aligned}$$

A simple reasoning shows that: $\mathcal{L}'v = \nu v'' - cv'$, and $D(\mathcal{L}') = D(\mathcal{L})$ (see [2, pp. 93-94] and [6, pp. 167-171, 276]). Let $u \in D(\mathcal{L}) = D(\mathcal{L}')$. Then we have

$$\begin{aligned}\|\mathcal{L}u\|^2 &= \int_0^d (\nu^2|u''(x)|^2 + c^2|u'(x)|^2 + 2\nu c(u''(x)\bar{u}'(x) + u'(x)\bar{u}''(x)))\, dx, \\ &= \nu^2\|u''\|^2 + c^2\|u'\|^2 + \nu c(|u'(d)|^2 - |u'(0)|^2), \\ \|\mathcal{L}'u\|^2 &= \int_0^d (\nu^2|u''(x)|^2 + c^2|u'(x)|^2 - 2\nu c(u''(x)\bar{u}'(x) + u'(x)\bar{u}''(x)))\, dx, \\ &= \nu^2\|u''\|^2 + c^2\|u'\|^2 - \nu c(|u'(d)|^2 - |u'(0)|^2).\end{aligned}$$

Let $u(x) = x^2(x-d)$, then $u \in D(\mathcal{L}) = D(\mathcal{L}')$. Moreover, $\|\mathcal{L}u\|^2 - \|\mathcal{L}u\|^2 = 2\nu c(|u'(d)|^2 - |u'(0)|^2) = 2\nu c d^4$. This implies that $\|\mathcal{L}u\|^2 \neq \|\mathcal{L}u\|^2$, and proves that $\mathcal{L}$ is *nonnormal*. In fact, we have $\mathcal{L}\mathcal{L}'u = \mathcal{L}'\mathcal{L}u = \nu^2 u^{(4)} - c^2 u^{(2)}$ for any function $u \in D(\mathcal{L}\mathcal{L}') \cap D(\mathcal{L}'\mathcal{L})$, but $D(\mathcal{L}\mathcal{L}') \neq D(\mathcal{L}'\mathcal{L})$. The following formulas give the domain of $\mathcal{L}\mathcal{L}'$ and of $\mathcal{L}'\mathcal{L}$:

$$\begin{aligned}D(\mathcal{L}\mathcal{L}') &= \{u^{(4)} \in L^2[0,\, d];\ u(0) = u(d) = 0,\ u''(0) = u'(0), \\ &\qquad \text{and } u''(d) = u'(d)\}, \\ D(\mathcal{L}'\mathcal{L}) &= \{u^{(4)} \in L^2[0,\, d];\ u(0) = u(d) = 0,\ u''(0) = -u'(0), \\ &\qquad \text{and } u''(d) = -u'(d)\},\end{aligned}$$

where $u^{(n)}$ denotes the $n^{\text{th}}$ derivative of the function $u$. An other way to show that $\mathcal{L}$ is a nonnormal operator is to show that its eigenfunctions are not orthogonal [7].

# 3 Pseudospectra of $\mathcal{L}$

Before discussing of the pseudospectra of the operator $\mathcal{L}$, we recall several equivalent definitions of the pseudospectra in the general case of a close linear operator $T$ in some Hilbert space $\mathcal{H}$. For more information about pseudospectra and the related literature, the reader is referred to [1, 10] and the papers cited in.

The following theorem is devoted to give four equivalent definitions of the pseudospectra. The proof and further comments are given in [4].

**Theorem 3.1** *Let $T$ be a closed linear operator in a Hilbert space $\mathcal{H}$ with a dense domain $D(T)$, and $\epsilon > 0$. Then the $\epsilon$-pseudospectrum $\sigma_\epsilon(T)$ satisfies the following equivalent definitions:*

$$\{z \in \mathbb{C} : \ \|(z-T)^{-1}\| \geq \frac{1}{\epsilon}\} \cup \sigma(T), \tag{6}$$

$$\{z \in \mathbb{C} : \ \exists\, (x_n)_{n\in\mathbb{N}} \in D(T), \|x_n\| = 1 \, \textit{for all}\ n \in \mathbb{N}\, \textit{and} \\ \lim_{n\to\infty} \|(z-T)x_n\| \leq \epsilon\} \cup \sigma(T), \tag{7}$$

$$\mathit{cl}(\{z \in \mathbb{C} : \ \exists x \in D(T), \ \|x\| = 1 \ \textit{and}\, \|(z-T)x\| < \epsilon\}) \cup \sigma(T), \tag{8}$$

$$\mathit{cl}(\{z \in \mathbb{C} : \ z \in \sigma(T+E) \ \textit{for some}\ E \in \mathcal{L}(\mathcal{H}) \ \textit{with}\, \|E\| \leq \epsilon\}), \tag{9}$$

*where $cl(S)$ of some set $S$ denotes the closure set of $S$, and $\sigma(T)$ denotes the spectrum of $T$.*

Computing the $\epsilon$-pseudospectrum is easier in the case of matrices than in the case of operators with infinite rank. In the case of a matrix $A \in \mathbb{C}^{n\times n}$, $\sigma_\epsilon(A)$ is given by formula (6): by calculating the resolvent norm $\|(z-A)^{-1}\|$ of $A$ in some grid points in a chosen complex region, and plotting the levels curves $\{z \in \mathbb{C} : \ \|(z-A)^{-1}\| = 1/\epsilon\}$ by using the contour plot of Matlab (see [1] and the papers cited in for more information); or by using the formula (9): by superposing the eigenvalues of $A + \epsilon E$ for a sufficiently large number of random complex matrices $E$ of norm 1. The final figure gives generally a good approximation of $\sigma_\epsilon(A)$ for all $\epsilon > 0$ [9].

Unfortunately, in the case of a closed linear operator $T$ of infinite dimension, the calculation of the pseudospectrum is very difficult if not impossible. This is due to:

1. the difficulty for computing of the resolvent norm $\|(z-T)^{-1}\|$ of $T$ for some $z$ with formula (6) ;

2. the difficulty for computing the norm of $(z-T)x$ for some $x \in D(T)$ with norm 1, and the fact that the unit disk $B = \{x \in \mathcal{H};\ \|x\| = 1\}$ is not a compact set so the infinity of choose of $x \in D(T) \cap B$ in the two formulas (7) and (8) ;

3. finally the difficulty for computing the spectrum of $T + \epsilon E$ for some bounded operator $E$ of norm 1, and the fact that the unit disk $S =$

$\{E \in \mathcal{L}(\mathcal{H});\ \|E\| = 1\}$ is not compact, and the difficulty of the choose of this $E$.

In a word, the formula (7), (8), and (9) are unusable at least in their current form. We will see later how to use slight modification of formula (8) to approximate the pseudospectra.

As mentioned above, the resolvent norm is very hard to find explicitly, and we have no way to calculate it. Moreover, the only thing that can be done is to approximate it over all data of the resolvent set. Here after, we will give two functions which bound above and below the resolvent norm over all data in the resolvent set of the operator $\mathcal{L}$.
The first natural idea is to bound the resolvent norm $\|(z - \mathcal{L})^{-1}\|$ of the operator $\mathcal{L}$ in some complex data $z$ in the resolvent set as follows:

$$\|(z - \mathcal{L})^{-1}\| = \|G_z\| \leq \|g_z\|_2 \tag{10}$$

where

$$\begin{aligned}
\|g_z\|_2 &= \left(\int_0^d \int_0^d |g_z(y, x)|^2 \, dx \, dy\right)^{1/2} \\
&= 2e^d |k|^{-2} [a_1^2 \cosh(d) - \frac{2da_r}{1 - a_r^2} \sinh(a_r d) - \frac{2da_i}{1 + a_i^2} \sin(a_i d) \\
&\quad - \frac{4(2a_r^4 - a_r^2 + a_i^2)}{(1 - a_r^2)^2 (a_r^2 + a_i^2)} \cosh(a_r d) - \frac{4(2a_i^4 - a_i^2 + a_r^2)}{(1 + a_i^2)^2 (a_r^2 + a_i^2)} \cos(a_i d)].
\end{aligned}$$

We note that the Green function $g_z$ is not defined in the spectrum $\sigma(\mathcal{L})$ of $\mathcal{L}$, since in Equation 5, we divide by some constant $k$ depending on the data $z$ and which is equal to zero in $\sigma(\mathcal{L})$.

The $\epsilon$-pseudospectrum of $\mathcal{L}$ is the set of all $z$ in the complex plan so that the resolvent norm is greater then $1/\epsilon$. (By convention we write $\|(zI - \mathcal{L})^{-1}\| = \infty$ if $\lambda$ is in the spectrum $\sigma(\mathcal{L})$ of $\mathcal{L}$.) Therefore, the upper bound of the resolvent norm gives us some set $\sigma_{s\epsilon}(\mathcal{L})$ for all $\epsilon > 0$, which contains the $\epsilon$-pseudospectrum $\sigma_\epsilon(\mathcal{L})$ of $\mathcal{L}$ ($\sigma_\epsilon(\mathcal{L}) \subseteq \sigma_{s\epsilon}(\mathcal{L})$). This set is defined as follows:

$$\sigma_{s\epsilon}(\mathcal{L}) \quad = \quad \{z \in \rho(\mathcal{L});\ \|g_z\|_2 \geq \frac{1}{\epsilon}\} \cup \sigma(\mathcal{L}). \tag{11}$$

where $\rho(\mathcal{L})$ is the resolvent set of $\mathcal{L}$.

The second idea is to reduce the norm of the resolvent, and to choose some function $f_z \in L^2[0,\ d]$ such that $\|(z-\mathcal{L})^{-1} f_z\| / \|f_z\| \simeq \|(z-\mathcal{L})^{-1}\|$ or equivalently some function $\Phi_z \in D(\mathcal{L})$ such that $\|\Phi_z\| / \|(z - \mathcal{L})\Phi_z\| \simeq \|(z - \mathcal{L})^{-1}\|$.

To this end, let $z \in \rho(\mathcal{L})$. If we omit the boundary condition $u(d) = 0$, then the function $\phi_z(x) = e^{\alpha_+ x} - e^{\alpha_- x}$ satisfies $(z - \mathcal{L})\phi_z = 0$, where the $\alpha_\pm$ are the solutions of the equation $z = \alpha^2 + \alpha$. Furthermore, if $z \in \{x + iy \in \mathbb{C};\ x < -y^2\}$, then $\phi_z(d) \ll 1$ for some $d$ sufficiently large [7], where the constant $\nu$ and $c$ is taken equal to 1. In the remaining of this paper, without further mention, we take $\nu$ and $c$ equal to 1, and $d$ equal to 40. A simple reasoning shows that if the function $\Phi_z$ is chosen of the form $\phi_z + \delta\phi_z$ such that $\Phi_z \in D(\mathcal{L})$, and $\delta\phi_z$ is a small perturbation so $\delta\phi_z''$ and $\delta\phi_z'$ remain small too, the function $\Phi_z$ can be a good one [7].

In the remaining, the function $\delta\phi_z$ is zero except in a small interval $[d - \frac{1}{k},\, d]$ ($k \gg 1$), in which $\delta\phi_z$ is a polynomial function of degree two so $\delta\phi_z''$ is in $L^2[0,\, d]$ and $\delta\phi_z(d) = -\phi_z(d)$. More precisely, $\delta\phi_z = -\varphi_k$ where

$$\varphi_k(x) = \phi_z(d) \begin{cases} 0 & \text{if } 0 \le x \le d - \frac{1}{k} \\ k^2(x - (d - \frac{1}{k}))^2 & \text{if } d - \frac{1}{k} \le x \le d. \end{cases}$$

We notice that $\varphi_k'(x) = 2\phi_z(d)k^2(x - (d - \frac{1}{k}))$ and $\varphi_k''(x) = 2\phi_z(d)k^2$ if $d - \frac{1}{k} < x < d$, 0 otherwise. And

$$(z - \mathcal{L})\Phi_z(x) \quad = \quad -z\varphi_k(x) + \varphi_k''(x) + \varphi_k'(x)$$

where $\Phi_z = \phi_z - \varphi_k$. The subscript $k$ of $\varphi_k$ is a constant taken equal to 100 and is not allowed to vary.

$$\begin{aligned}
\|(z - \mathcal{L})\Phi_z\|^2 &= \|z\varphi_k - \varphi_k'' - \varphi_k'\|^2, \\
&= \int_{d-\frac{1}{k}}^{d} |z\varphi_k(x) - \varphi_k''(x) - \varphi_k'(x)|^2\, dx, \\
&= k^4|\phi_z(d)|^2 \int_0^{\frac{1}{k}} |zx^2 - 2x - 2|^2\, dx, \\
&= |\phi_z(d)|^2\Big(\frac{|z|^2}{5k} - Re\, z(1 + \frac{4}{3}k) + \frac{4}{3}k + 4k^2 + 4k^3\Big).
\end{aligned}$$

Let $a + i\, b = \frac{1}{2}\sqrt{1 + 4z}$, therefore

$$\begin{aligned}
\|\Phi_z\|^2 \;\simeq\; \|\phi_z\|^2 &= \int_0^d |\phi_z(x)|^2\, dx, \\
&= 2\left(\frac{e^{-d}(\cosh(ad) + a\sinh(ad)) - 1}{a^2 - 1} + \frac{e^{-d}(\cos(bd) - b\sin(bd)) - 1}{1 + b^2}\right).
\end{aligned}$$

So, the resolvent norm $\|(z - \mathcal{L})^{-1}\|$ is bounded below as follows:

$$\|(z - \mathcal{L})^{-1}\| \;\geq\; \frac{\|\Phi_z\|}{\|(z - \mathcal{L})\Phi_z\|},$$

where $\Phi_z$ is defined above for all $z$ in the resolvent set. This lower bound of the resolvent norm $\|(z-\mathcal{L})^{-1}\|$ gives us some set $\sigma_{m\epsilon}(\mathcal{L})$ included in the $\epsilon$-pseudospectrum $\sigma_\epsilon(\mathcal{L})$ for all $\epsilon > 0$ ($\sigma_{m\epsilon}(\mathcal{L}) \subseteq \sigma_\epsilon(\mathcal{L})$). This set, $\sigma_{m\epsilon}(\mathcal{L})$, is defined by follows:

$$\sigma_{m\epsilon}(\mathcal{L}) \quad = \quad \{z \in \mathbb{C};\ \frac{\|\Phi_z\|}{\|(z-\mathcal{L})\Phi_z\|} \geq \frac{1}{\epsilon}\} \cup \sigma_\epsilon(\mathcal{L}). \tag{12}$$

Now, we have two sets $\sigma_{m\epsilon}(\mathcal{L})$ and $\sigma_{s\epsilon}(\mathcal{L})$ which respectively includes and contains $\sigma_\epsilon(\mathcal{L})$ for all $\epsilon > 0$ ($\sigma_{m\epsilon}(\mathcal{L}) \subseteq \sigma_\epsilon(\mathcal{L}) \subseteq \sigma_{s\epsilon}(\mathcal{L})$). Unfortunately, these two sets are quite different and at least one of them does not give a good approximation about the $\epsilon$-pseudospectrum of $\mathcal{L}$. We anticipate that $\sigma_{m\epsilon}(\mathcal{L})$ approximates $\sigma_\epsilon(\mathcal{L})$ more accurately than $\sigma_{s\epsilon}(\mathcal{L})$.

The formula defining the two sets $\sigma_{m\epsilon}(\mathcal{L})$ and $\sigma_{s\epsilon}(\mathcal{L})$ are complex. Moreover, it is difficult to foresee the shape of $\sigma_{m\epsilon}(\mathcal{L})$ and $\sigma_{s\epsilon}(\mathcal{L})$, and even more the shape of $\sigma_\epsilon(\mathcal{L})$ which lives between the two sets. It is very likely that the pseudospectra of $\mathcal{L}$ approximates a parabolic region in the left half-plane as $\sigma_{m\epsilon}(\mathcal{L})$ and $\sigma_{s\epsilon}(\mathcal{L})$ do, in the neighborhood of zero. But, $\sigma_\epsilon(\mathcal{L})$ can not have exactly the form of a parabolic region. In fact, it behaves like an ellipse with the main axis in the negative real axis, plus some other sets like disks centered on the negative eigenvalues of $\mathcal{L}$ with large module. In fact, the operator $\mathcal{L}$ is similar to a self-adjoint operator: $\mathcal{L} = \mathcal{M}\mathcal{K}\mathcal{M}^{-1}$ where $\mathcal{K}$ is a self-adjoint operator, and $\mathcal{M}$ is invertible, and defined by (see [6, Example III.6.11] and [7, pp. 16-19]):

$$\mathcal{K}v = v'' - \frac{1}{4}v, \quad \mathcal{M}v = e^{-\frac{x}{2}}v, \text{ and } \mathcal{M}^{-1}v = e^{\frac{x}{2}}v.$$

We note that $\|\mathcal{M}\| = 1$, $\|\mathcal{M}^{-1}\| = e^{d/2}$, and

$$\begin{aligned} \|(z-\mathcal{L})^{-1}\| \quad &= \quad \|\mathcal{M}(z-\mathcal{K})^{-1}\mathcal{M}^{-1}\| \ \leq \ \|\mathcal{M}\|\,\|\mathcal{M}^{-1}\|\,\|(z-\mathcal{K})^{-1}\| \\ &= \quad \frac{\kappa(\mathcal{M})}{\text{dist}(z, \sigma(\mathcal{L}))} \end{aligned} \tag{13}$$

where $\kappa(\mathcal{M}) = \|\mathcal{M}\|\,\|\mathcal{M}^{-1}\|$. We recall that $\sigma(\mathcal{K}) = \sigma(\mathcal{L})$, and $\|(z-\mathcal{K})^{-1}\| = 1/\text{dist}(z, \sigma(\mathcal{K}))$ since $\mathcal{K}$ is a self-adjoint operator. Formula (13) implies that

$$\sigma_\epsilon(\mathcal{L}) \ \subseteq \ \bigcup_{n\in\mathbb{N}} D(\lambda_n, \epsilon\kappa(\mathcal{M})) \tag{14}$$

where $D(\lambda_n, \epsilon\kappa(\mathcal{M})$ is the disk of radius $r = \epsilon\kappa(\mathcal{M})$ and centered on the eigenvalues $\lambda_n = -1/4 - \pi^2 n^2/d^2$ of $\mathcal{L}$ for all $n \in \mathbb{N}$. However the distance

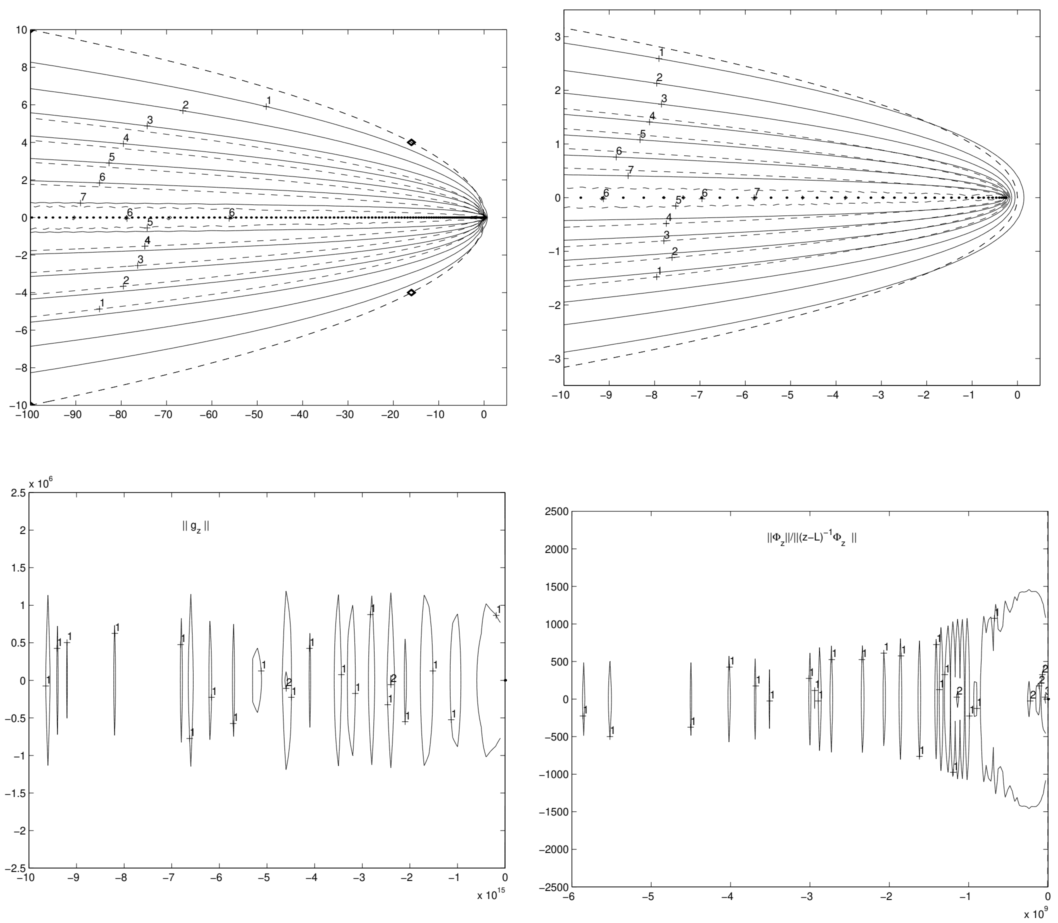


Figure 1: *The $\epsilon$-pseudospectra of the convection-diffusion operator $\mathcal{L}$ is not known exactly. The dashed curves (resp., the solid curves) are the boundary of $\sigma_{m\epsilon}(\mathcal{L})$ (resp., $\sigma_{s\epsilon}(\mathcal{L})$) defined by* (12) *(resp.,* (11)*) and are reported for all $\epsilon = 10^{-1}$, $10^{-2}$, ... , $10^{-7}$. We recall that $\sigma_{m\epsilon}(\mathcal{L}) \subseteq \sigma_{\epsilon}(\mathcal{L}) \subseteq \sigma_{s\epsilon}(\mathcal{L})$.*

between two successive eigenvalues $|\lambda_{n+1}-\lambda_n| = \pi^2(2n+1)/d^2$ becomes larger and larger when $n$ increases ($|\lambda_{n+1}-\lambda_n| \to \infty$ when $n \to \infty$). Therefore, for all $\epsilon > 0$ there exists $n_\epsilon \geq 0$ such that, for all $n \geq n_\epsilon$, the disk $D(\lambda_n, \epsilon\kappa(\mathcal{M}))$ is separated from the other disks with same radius and centered on the other eigenvalues of $\mathcal{L}$. Moreover, we note that the eigenvalues of largest modulus are more stable than eigenvalues of with smallest module (see Figure 1).

The following section describes the pseudospectra of the discretized matrices and compare them with the two sets $\sigma_{m\epsilon}(\mathcal{L})$ and $\sigma_{s\epsilon}(\mathcal{L})$ are traced.

# 4 Figures

Figure 1 is devoted to display the two approximations $\sigma_{m\epsilon}(\mathcal{L})$ and $\sigma_{s\epsilon}(\mathcal{L})$ which respectively are included in and contains the $\epsilon$-pseudospectra of $\mathcal{L}$. The values of $\|\Phi_z\|/\|(z-\mathcal{L})\Phi_z\|$ (resp., $\|g_z\|$) are computed on $100 \times 100$ grid points. The resulting array is then fed to the contour plot of Matlab. We note that, here and in all our further experiments, the constants $d$, $\nu$ and $c$ of the formula (1) are respectively equal to 40, 1 and 1. The dashed level curves $\|\Phi_z\|/\|(z-\mathcal{L})\Phi_z\| = 1/\epsilon$ (resp., solid lines $\|g_z\| = 1/\epsilon$) are plotted for all $\epsilon = 10^{-1}, \ldots, 10^{-7}$. The points appearing on the negative real axis are the exact eigenvalues of $\mathcal{L}$ located in the region of interest. The outward dashed curve (which is not numbered) is the parabola $x = -y^2$. We note that the field of values $W(\mathcal{L}) = \{(\mathcal{L}x, x)/\|x\|^2;\ x \in D(\mathcal{L}),\ x \neq 0\}$ is included in $\mathcal{P} = \{x + iy \in \mathbb{C};\ x \leq -y^2\}$ [7]. $\mathcal{P}$ is the region enclosed by the parabola.

All the other figures are devoted to display the spectrum and the pseudospectrum of the discretized matrices of the operator $\mathcal{L}$. Let us denote these matrices by $A_N$ for the moment. The $\epsilon$-pseudospectrum $\sigma_\epsilon(A_N)$ of the all matrix $A_N$ is plotted for all $\epsilon = 10^{-1}, 10^{-2}, \ldots, 10^{-7}$. The resolvent norm $\|(z - A_N)^{-1}\|$ is computed on $50 \times 50$ grid points, and the resulting array are than fed to the contour plot of Matlab, for all cases of discretization schemes. The eigenvalues of the matrices $A_N$ are denoted by a + sign. The parabola $x = -y^2$ is again plotted. [1]

The rest of this part is devoted to the approximation of the convection-diffusion operator $\mathcal{L}$ by finite difference and spectral method. The spectrum and pseudospectrum of the resulting matrices were studied and presented in every case.

We notice that the pseudospectra of the resulting matrices approximate locally in the neighborhood of zeros the pseudospectra of $\mathcal{L}$. This approximation becomes less accurate when we get slightly away from zero. Moreover, the accuracy of these approximations depends strongly on the discretization scheme. But, a point with a large modulus in $\sigma_\epsilon(\mathcal{L})$ requires a very large order $N$ of discretization to be in the $\sigma_\epsilon(A_N)$ for some discretized matrix $A_N$.

[1]'Figures 3 and 5' appeared in [7].

# 5 Finite Difference

The simple three-point-centered finite difference is used to approximate the convection-diffusion operator $\mathcal{L}$ in (1). Two sets of points are used: in the first subsection, we use Chebyshev points, in the second one, equidistant points. In each case, the convection-diffusion operator $\mathcal{L}$ with the Dirichlet boundary condition $u(0) = u(d) = 0$ is approximated by a tridiagonal matrix of order $N - 1$. We note these matrices by $L_N^{fed}$ when the equidistant points are used and by $L_N^{fch}$ in the case of Chebyshev ones. The spectrum and the pseudospectrum are reported in each case. We note that the spectrum and the pseudospectrum in the case of equidistant points is more accurate than in the case of Chebyshev ones.

## 5.1 Chebyshev Points

The simple three-point-centered finite difference scheme with Chebyshev points $x_n = (d/2)(1 - \cos(n\pi/N))$ for all $1 \leq n \leq N$ to approximate the operator $\mathcal{L}$ defined by (1) yields a tridiagonal matrix $L_N^{fch}$ of order $N - 1$. We recall that in this case the first derivative $u'(x_n)$ and the second ones $u''(x_n)$ are approximated as follows:

$$\begin{aligned}
u'(x_n) &= \frac{u_{n+1} - u_{n-1}}{x_{n+1} - x_{n-1}};\\
u''(x_n) &= 2\frac{(x_n - x_{n-1})u_{n+1} - (x_{n+1} - x_{n-1})u_n + (x_{n+1} - x_n)u_{n-1}}{(x_{n+1} - x_n)(x_n - x_{n-1})(x_{n+1} - x_{n-1})},
\end{aligned}$$

for all $1 \leq n \leq N - 1$ where $u_n = u(x_n)$. So, the entries of the matrix $L_N^{fch}$ are

$$\begin{aligned}
l_{nn+1} &= \frac{2}{(x_{n+1} - x_n)(x_{n+1} - x_{n-1})} + \frac{1}{x_{n+1} - x_{n-1}};\\
l_{nn-1} &= \frac{2}{(x_n - x_{n-1})(x_{n+1} - x_{n-1})} - \frac{1}{x_{n+1} - x_{n-1}};\\
l_{nn} &= -\frac{2}{(x_{n+1} - x_n)(x_n - x_{n-1})} \qquad \text{for all } 1 \leq n \leq N - 1.
\end{aligned}$$

We notice that the matrix $L_N^{fch}$ is not symmetric and is not a Toeplitz matrix. And in this case, we do not have an explicit formula of the eigenvalues of the matrix $L_N^{fch}$ as in the case of equidistant points.

In Figure 2, we display the spectra and the pseudospectrum of the matrix $L_{30}^{fch}$ in the upper part, and those of $L_{150}^{fch}$ in the lower part. We note that

$\sigma_\epsilon(L_N^{fch})$ does not extend in width: all $\lambda \in \sigma_{10^{-1}}(L_{150}^{fch})$ have an imaginary part does not go beyond 4 in absolute value, limiting the accuracy of the approximation.

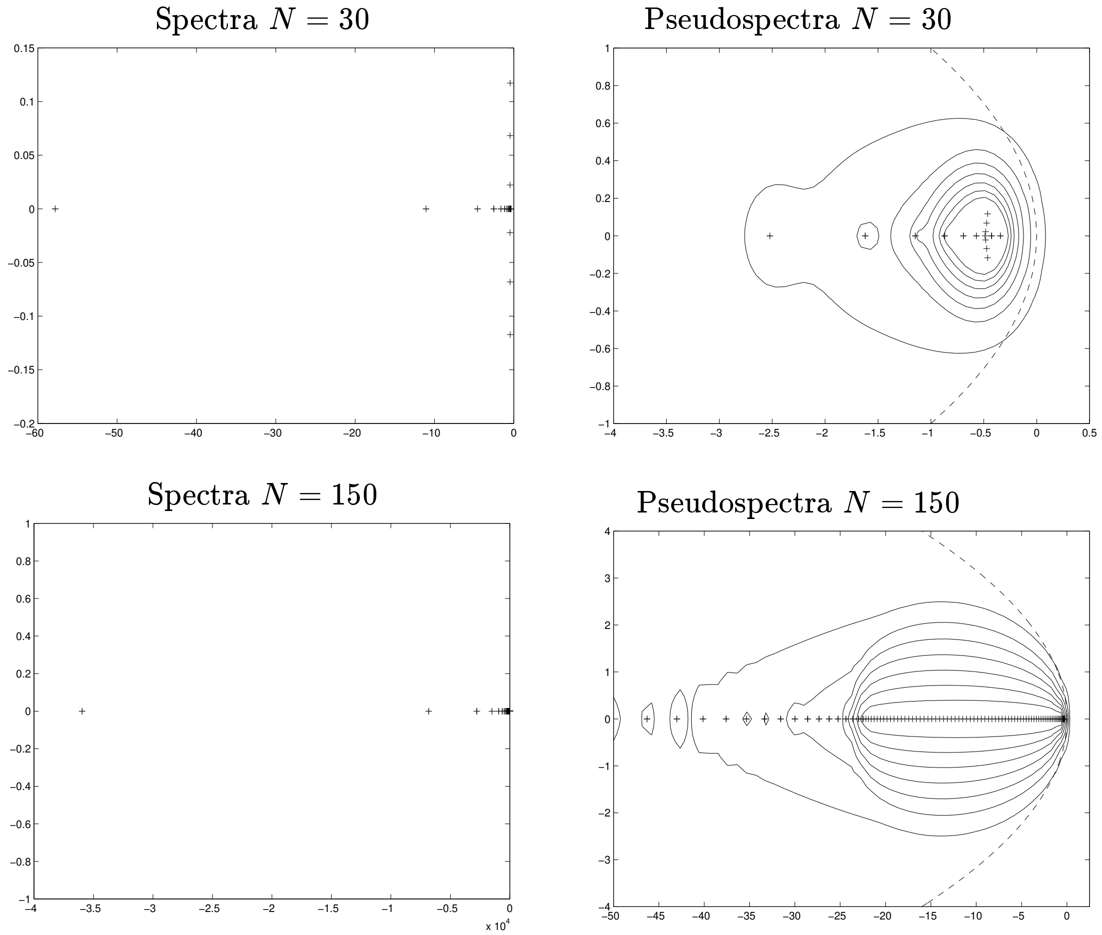


Figure 2: *The matrices $L_N^{fch}$ approximating the 1D convection-diffusion operator* (1) *by centered finite difference and Chebyshev points.* $\|L_{30}^{fch}\|_2 = 58.7540$, $\|L_{150}^{fch}\|_2 = 3.6232e+04$.

## 5.2 Equidistant Points

The simple three-point-centered finite difference is used to approximate the convection-diffusion operator $\mathcal{L}$ in (1) in the equidistant points.
Let $N > 1$ and $h = d/N$. The equidistant points are $x_j = jh$ for all

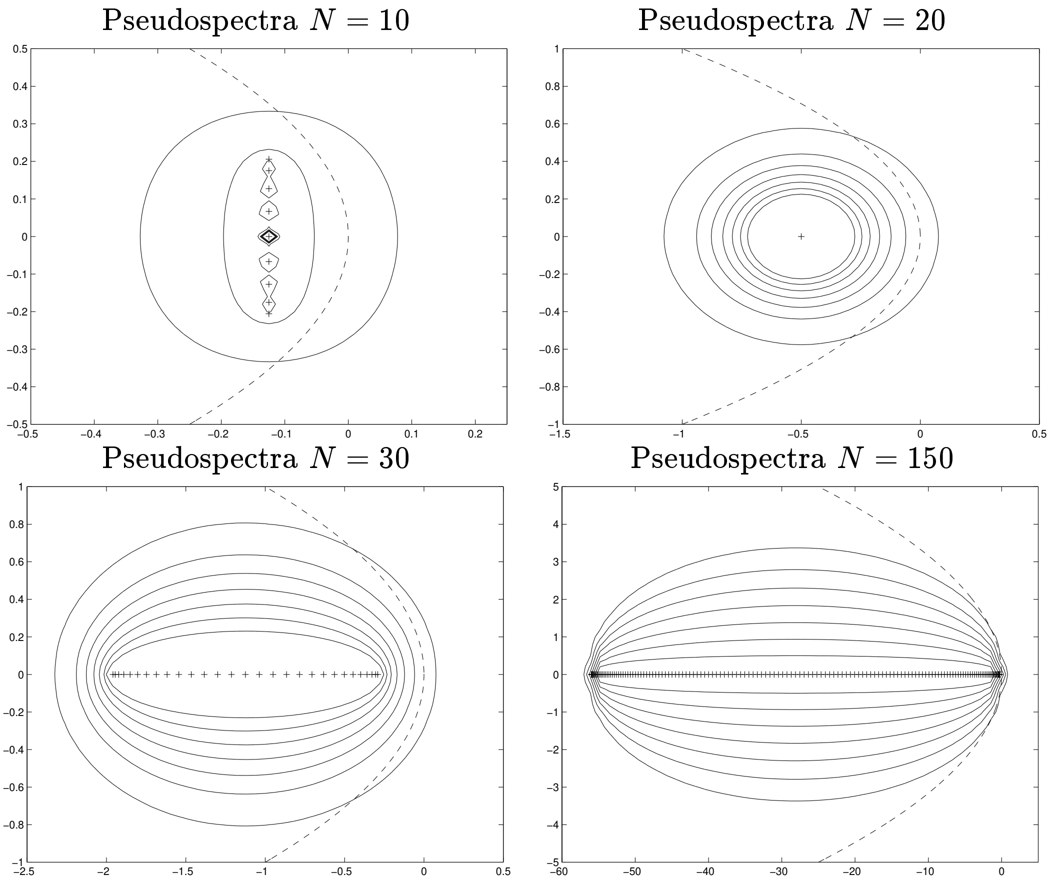


Figure 3: *The matrices $L_N^{fed}$ approximating the 1D convection-diffusion operator* (1) *by centered finite difference and equidistant points.* $\|L_{10}^{fed}\|_2 = 0.2821$, $\|L_{20}^{fed}\|_2 = 0.9968$, $\|L_{30}^{fed}\|_2 = 2.2451$ *and* $\|L_{150}^{fed}\|_2 = 56.2439$.

$j = 0, 1, \ldots, N$. The second and first derivative are approximated as follows:

$$u''(x_j) \approx \frac{u(x_{j+1}) - 2u(x_j) + u(x_{j-1})}{h^2}, \qquad u'(x_j) \approx \frac{u(x_{j+1}) - u(x_{j-1})}{2h}.$$

The centered finite difference scheme for the convection-diffusion operator $\mathcal{L}$ as described above yields a tridiagonal Toeplitz matrix $L_N^{fed}$ of order $N-1$ and entries

$$l_{j\,j} = \frac{-2\nu}{h^2}, \qquad l_{j\,j\pm1} = \frac{\nu}{h^2} \pm \frac{c}{2h} \qquad \text{for all} \qquad 1 \le j \le N-1.$$

Let the Péclet number be $Pe = cd/\nu$, and the discretized Péclet number $\overline{Pe} = Pe/2N = cd/(2N\nu)$. We notice that the discretized Péclet number decreases linearly as a function of $N$. We can write

$$L_N^{fed} = \frac{\nu}{h^2}\begin{pmatrix} -2 & 1+\overline{Pe} & & & \\ 1-\overline{Pe} & -2 & 1+\overline{Pe} & & \\ & \ddots & \ddots & \ddots & \\ & & 1-\overline{Pe} & -2 & 1+\overline{Pe} \\ & & & 1-\overline{Pe} & -2 \end{pmatrix}.$$

The eigenvalues of a tridiagonal Toeplitz matrix are known explicitly (see [5, pp. 524-525] and the reference in it to explicit formulas). For the matrix $L_N^{fed}$, the eigenvalues $(\lambda_k)_{k=1,\dots,N-1}$ are:

$$\lambda_k = -\frac{2\nu}{h^2} + 2(\frac{\nu^2}{h^4} - \frac{c^2}{4h^2})^{\frac{1}{2}}\cos(\frac{k\pi}{N-1}) \qquad \text{for all } k = 1, 2, \dots, N-1,$$

or equivalently,

$$\lambda_k = -2\frac{\nu}{h^2}(1 - \sqrt{1-\overline{Pe}}\cos(\frac{k\pi}{N-1})) \quad \text{for all } k = 1, 2, \dots, N-1. \quad (15)$$

The three following cases are imposed:

1. If $\overline{Pe} > 1$ (the order of discretization $N$ is less than $Pe/2$). The eigenvalues of $L_N^{fed}$ are simple points in the the vertical line $\{-2\nu/(h^2) + iy;\ y \in \mathbb{R}\}$ where $i = \sqrt{-1}$. The matrix $L_N^{fed}$ is diagonalizable.

2. If $\overline{Pe} = 1$ (the order of discretization $N$ is equal to $Pe/2$), the eigenvalues of $L_N^{fed}$ collapse at $\frac{-2\nu}{h^2}$. The matrix $L_N^{fed}$ is equivalent to one Jordan bloc of order $N-1$.

3. If $\overline{Pe} < 1$ (the order of discretization $N$ is largerthan $Pe/2$). The eigenvalues of $L_N^{fed}$ are negative real and simple. The matrix $L_N^{fed}$ is diagonalizable.

The most important case is evidently when $N$ is large, more precisely $N \gg Pe/2$, so, $\overline{Pe} \ll 1$. In this case, the spectrum and the pseudospectrum of $L_N^{fed}$ give more information about those of the operator $\mathcal{L}$ as expected.

In summary, these matrices are tridiagonal Toeplitz matrices, there eigenvalues are known explicitly. Moreover we can have some approximation of there pseudospectra [8].

In Figure 3, we show the spectrum and the pseudospectrum of four matrices $L_N^{fed}$ for four values of $N$ as follows: in the upper left corner $N = 10$, the upper right corner $N = 20$, the lower left corner $N = 30$, and in the lower right corner $N = 150$. (The eigenvalues are marked as usual by $+$ points.)

We notice that for $N = 10$, corresponding to $N < Pe/2 = d/2$, the eigenvalues of $L_{10}^{fed}$ are on a vertical line (here and after, $d = 40$, and $c = \nu = 1$). For $N = 20$, corresponding to $N = Pe/2$, the eigenvalues of $L_{20}^{fed}$ collapse in one point, and for $N = 30$ or $150$ corresponding to $N > Pe/2$, the eigenvalues of $L_{30}^{fed}$, $L_{150}^{fed}$ are distinct and on the negative real axis.

As expected the spectrum and the pseudospectrum of the matrix $L_N^{fed}$ approximate more and more accurately those of the operator $\mathcal{L}$ when the order of discretization becomes larger. Unfortunately, the $\epsilon$-pseudospectra of $L_N^{fed}$ remain small and do not extend very well in the region $\mathcal{P}$ bounded by the parabola $\{x = -y^2\}$ as $\sigma_\epsilon(\mathcal{L})$ does.

# 6 Spectral Method

This section is devoted to the study of the spectral method to approximate the convection-diffusion operator $\mathcal{L}$ defined by (1). In the first subsection, the collocation approximation is used. The collocation points are the Chebyshev ones, which are more accurate than the equidistant ones as explained below. In the second subsection the Galerkin approximation is used. The sine functions are chosen as basis functions.

In the Galerkin-Fourier approximation, the operator $\mathcal{L}$ is approximated by a matrix $L_N^{GF}$ of order $N$, and in the collocation approximation by a matrix $L_N^{CC}$ of order $N - 1$. The spectrum and the pseudospectrum of the last matrices are presented in the two cases.

We notice that the spectra of the matrix $L_N^{GF}$ given from the Galerkin-Fourier approximation is less accurate than the one resulting from the collocation approximation. In contrast, $\sigma_\epsilon(L_N^{GF})$ is slightly more accurate than $\sigma_\epsilon(L_N^{CC})$.

The spectrum of the matrix $L_N^{GF}$ obtained by Galerkin approximation is far from that of the operator $\mathcal{L}$. (We recall that the spectrum of the operator $\mathcal{L}$ is a discrete subset of the negative real axis.) The spectrum of $L_N^{GF}$ is located near the parabola $\{x = -y^2\}$ as indicated in Figure 6.

In contrast, most of the eigenvalues of the matrix $L_N^{CC}$ obtained by collocation approximation are on the negative real axis. Moreover, the imaginary part of the eigenvalues which are not on the real axis remain smaller (see Figure 5).

## 6.1 Collocation Approximation

In this subsection, the collocation approximation is used to approximate the convection-diffusion operator $\mathcal{L}$ defined by (1). The Chebyshev points $x_n = (d/2)(1 - \cos(n\pi/N))$ for all $n = 0, 1, \ldots, N$ are used as collocation points. These points were preferred to the equidistant ones for two reasons. The first one is that the matrices $L_N^{CC}$ given by the use of Chebyshev points are more accurate than the ones given by the equidistant ones. The second is that the Lagrange polynomial $l_n(x) = \prod_{m=0, m\neq n}^{N}(x - x_m)/(x_n - x_m)$ is highly unstable to perturbation when the equidistant points are used. Moreover, the Lagrange polynomial $l_n(x)$ with the use of equidistant points can take values of the order of $10^{33}$ for some moderate value of $N$ ($N = 150$) which can make the computation very unstable. In contrast the polynomials given by the use of Chebyshev points are more stable. Figure 4 below plots the Lagrange polynomial with Chebyshev and equidistant points for $N = 150$, and $n = 100$.

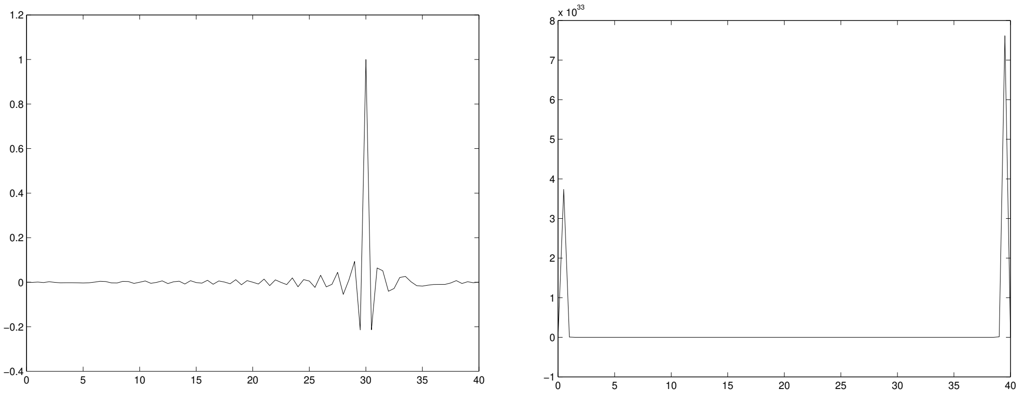

Figure 4: *The Lagrange polynomials in* $[0,\ 40]$ $l_j = \prod_{k=1,\, k\neq j}^{150} \frac{x - x_k}{x_j - x_k}$ *here* $j = 100$. *On the left side the* $(x_k)_{k=0,\ldots,150}$ *are the Chebyshev points ; on the right side the equidistant ones.*

Let $L_N^{CC}$ be the matrix given by collocation approximation of the convection-diffusion operator $\mathcal{L}$ with $N$ Chebyshev points as collocation points and the Lagrange polynomial as basis function. The order of $L_N^{CC}$ is $N - 1$, and its entries are:

$$l_{ij} = l_j''(x_i) + l_j'(x_i) \quad \text{for all} \quad 1 \leq i, j \leq N - 1.$$

In the upper part of Figure 5, we display the spectrum and the pseudospectrum of the approximate matrix $L_{30}^{CC}$ of order 30, those of $L_{150}^{CC}$ are in the middle. Two zooms of the pseudospectrum of $L_{150}^{CC}$ are in the lower part. We notice that only the smallest eigenvalues are highly unstable. The rest of the spectrum is stable, so only the sensitive part of the pseudospectra is given.

We judge that the pseudospectrum of the matrix $L_N^{CC}$ approximates very well the pseudospectrum of the operator $\mathcal{L}$ locally in the neighborhood of zero. Unfortunately, $\sigma_\epsilon(L_N^{CC})$ does not extend very well in the region $\mathcal{P}$ bounded by the parabola $\{x = -y^2\}$ as $\sigma_\epsilon(\mathcal{L})$ does.

## 6.2 Galerkin Fourier approximation

We recall that the Fourier sine basis $(\sqrt{2/d}\ \sin k\pi x/d)_{k\in\mathbb{N}-\{0\}}$ ; the Fourier cosine basis $(\sqrt{2/d}\ \cos k\pi x/d)_{k\in\mathbb{N}}$ and the Fourier basis $(\sqrt{2/d}\ e^{-2ik\pi x/d})_{k\in\mathbb{Z}}$ are Hilbert basis of $L^2[0,\ d]$.

We will use the Fourier sine basis which satisfy the boundary condition $u(0) = u(d) = 0$. We notice that for all function $u \in L^2[0,\ d]$, $u(x) = \sqrt{2/d}\ \sum_{n=1}^{\infty} u_n\ \sin(n\pi x/d)$ where $u_n = \sqrt{\frac{2}{d}} \int_0^d u(t)\sin(n\pi t/d)\,dt$. Moreover, the equality between $u$ and its Fourier sine series does not hold pointwise, but holds in $L^2[0,\ d]$.

The Galerkin Fourier approximation of the convection-diffusion operator $\mathcal{L}$ with Dirichlet boundary conditions $u(0) = u(d) = 0$ consists in finding some approximation operator $L_N^{GF} = I\!P_N \mathcal{L} I\!P_N$ where $I\!P_N$ is the orthogonal projection in the subspace $\mathcal{W}_N$ of $L^2[0,\ d]$ spanned by $\sin(n\pi x/d)$ for all $1 \le n \le N$ where $N$ is some positive integer.

To find an explicit formula of the operator $L_N^{GF}$, let $u$ be the function $\sqrt{2/d}\sum_{k=1}^{\infty} u_k \sin(k\pi x/d)\ \in L^2[0,\ d]$. Therefore

$$u'(x) = \frac{\pi\sqrt{2}}{d\sqrt{d}}\sum_{k=1}^{\infty} k u_k\ \cos(\frac{k\pi x}{d}), \qquad u''(x) = -\frac{\pi^2\sqrt{2}}{d^2\sqrt{d}}\sum_{k=1}^{\infty} k^2 u_k\ \sin(\frac{k\pi x}{d}).$$

We know that (see [3])

$$\cos(\frac{l\pi x}{d}) \quad = \quad \frac{4}{\pi} \sum_{\substack{k=1 \\ k+l,\ \mathrm{odd}}}^{\infty} \frac{k}{(k^2 - l^2)}\ \sin(\frac{k\pi x}{d}).$$

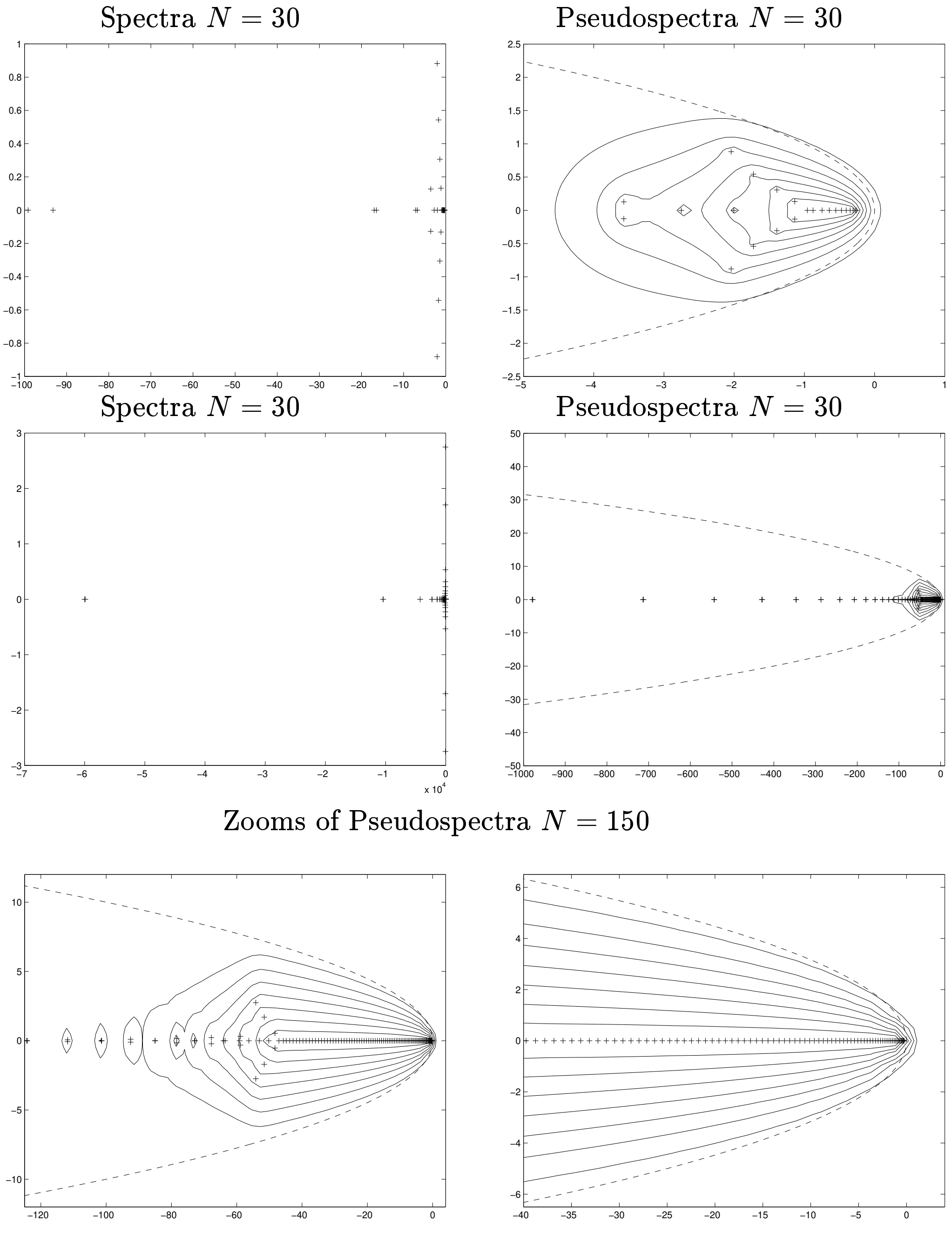


Figure 5: *The matrix* $L_N^{CC}$ *of order* $N$ *approximating the 1D convection-diffusion operator* (1) *by spectral collocation approximation and Chebyshev points.* $\|L_{30}^{CC}\| \simeq 100$, $\|L_{150}^{CC}\| \simeq 6 \times 10^4$.

Then

$$\begin{aligned}
\mathcal{L}u(x) &= u''(x) + u'(x), \\
&= -\frac{\pi^2 2^{1/2}}{d^{5/2}} \sum_{k=1}^{\infty} k^2 u_k \sin(\frac{k\pi x}{d}) + \frac{\pi 2^{1/2}}{d^{3/2}} \sum_{l=1}^{\infty} l u_l \cos(\frac{l\pi x}{d}), \\
&= \sum_{k=1}^{\infty} [-\frac{\pi^2 k^2 u_k}{d^2} + \frac{2^2}{d} \sum_{\substack{l=1 \\ k+l,\, \mathrm{odd}}}^{\infty} \frac{lk}{k^2 - l^2} u_l] \sqrt{\frac{2}{d}}\, \sin(\frac{k\pi x}{d}).
\end{aligned}$$

And

$$\begin{aligned}
L_N u(x) &= I\!P_N \mathcal{L} I\!P_N u(x), \\
&= I\!P_N(u_N''(x) + u_N'(x)) \text{ where } u_N(x) = I\!P_N u(x) = \sum_{k=1}^{N} u_k \sin(\frac{k\pi x}{d}), \\
&= I\!P_N(-\frac{\pi^2 2^{1/2}}{d^{5/2}} \sum_{k=1}^{N} k^2 u_k \sin(\frac{k\pi x}{d}) + \frac{\pi 2^{1/2}}{d^{3/2}} \sum_{l=1}^{N} l u_l \cos(\frac{l\pi x}{d})), \\
&= \sum_{k=1}^{N} [-\frac{\pi^2 k^2 u_k}{d^2} + \frac{2^2}{d} \sum_{\substack{l=1 \\ k+l,\, \mathrm{odd}}}^{N} \frac{lk}{k^2 - l^2} u_l] \sqrt{\frac{2}{d}}\, \sin(\frac{k\pi x}{d}).
\end{aligned}$$

Let $\mathcal{I}$ be the application of $L^2[0,\ d]$ in $l^2$ defined as follows

$$\begin{aligned}
\mathcal{I} \,:\, L^2[0,\ d] &\longrightarrow l^2 \\
f = \sum_{k=1}^{\infty} f_k \sqrt{\frac{2}{d}} \sin(\frac{k\pi x}{d}) &\mapsto \quad f = (f_k)_{k=1,2,\ldots}.
\end{aligned}$$

The application $\mathcal{I}$ is an isometry since $(\sqrt{\frac{2}{d}} \sin(\frac{k\pi x}{d}))_{k=1,2,\ldots}$ is a Hilbert basis of $L^2[0,\ d]$.

So, the convection-diffusion operator $\mathcal{L}$ on $L^2[0,\ d]$ defined by (1) can be considered as an operator on $l^2$, more precisely as an infinite matrix $L^{GF}$ with entries $(l_{ij})_{1 \le i,j \le \infty}$ where

$$l_{ij} = \begin{cases} -\frac{\pi^2 i^2}{d^2} & \text{if } j = i \\ \frac{2^2 i j}{d(i^2 - j^2)} & \text{if } j + i \ \text{ odd} \\ 0 & \text{otherwise.} \end{cases}$$

Similarly the approximate operator $L_N^{GF}$ can be viewed as a matrix of order $N$, which we also denote by $L_N^{GF}$. The matrix $L_N^{GF} = (l_{ij})_{1 \le i,j \le N}$ is the restriction of $L^{GF}$ in $\mathbb{C}^{N\times N}$. We notice that the operator $L^{GF}$ is closed and is not bounded in $l^2$ as the convection-diffusion operator $\mathcal{L}$ in $L^2[0,\,d]$.

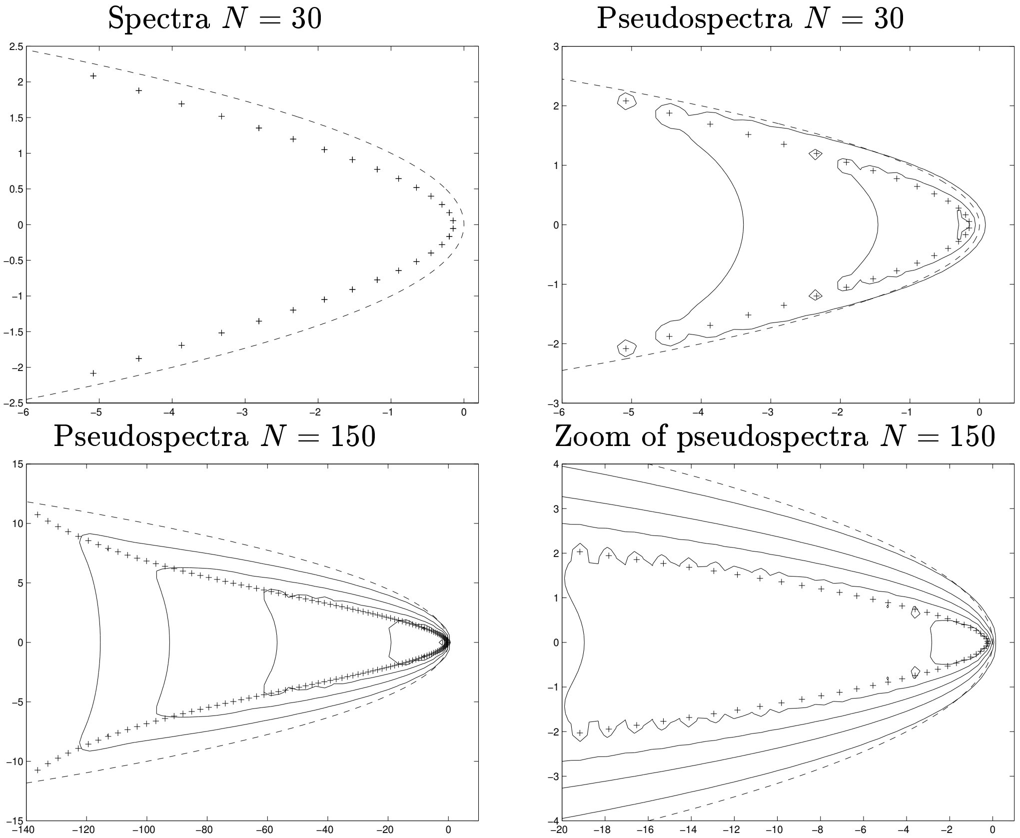


Figure 6: *The matrix* $L^{GF}_N$ *of order* $N$ *approximating the 1D convection-diffusion operator* (1) *by Galerkin approximation with the use of sine basis.* $\|L^{GF}_{30}\| \simeq 6$, $\|L^{GF}_{150}\| \simeq 139$.

We show in Figure 6 the spectrum and the pseudospectrum of the matrix $L^{GF}_{30}$ of order 30 approximating the operator $\mathcal{L}$ by Galerkin Fourier approximation in the upper part. In the lower one, the pseudospectrum of the matrix $L^{GF}_{150}$ and a zoom are displayed.

We notice that the spectrum of the matrices $L^{GF}_N$ is located near the parabola $\{x = -y^2\}$, and the pseudospectrum of these matrices approximate the region $\mathcal{P}$ bounded by the parabola. This is not by chance and comes from the fact that the operator $\mathcal{L}$ has a pseudospectrum approximating the region $\mathcal{P}$ and is a highly non-normal operator.

## References


[1] F. Chaitin-Chatelin and V. Frayssé. *Lectures on Finite Precision Computations.* SIAM, Philadelpha, 1996.

[2] F. Chatelin. *Spectral Approximation of Linear Operators.* Academic Press, New York, 1983.

[3] D. Gottlib and S. A. Orszag. *Numerical Analysis of Spectral Methods : Theory and Applications.* SIAM-CBMS, Philadelpha, 1977.

[4] A. Harrabi. On the approximation of pseudospectra of nonnormal operators by discretization part I: the first derivative operator. To appear as a Technical report at CERFACS, 1997.

[5] N. Higham. *Accuracy and Stability of Numerical Algorithms.* SIAM, Philadelphia, 1996.

[6] T. Kato. *Perturbation Theory for Linear Operators.* Springer, New York, 1976.

[7] S. C. Reddy and L. N. Trefethen. Pseudospectra of the convection-diffusion operator. *SIAM J. Appl. Math.*, 54:1634–1649, 1994.

[8] L. Reichel and L. N. Trefethen. Eigenvalues and pseudo-eigenvalues of Toeplitz matrices. *Linear algebra and its applications*, 162-164:153–185, 1992.

[9] L. N. Trefethen. Pseudospectra of matrices. In Numerical Analysis 1991, editor, *Longman, Harlow.* D. F. Griffiths and G. A. Watson, 1992.

[10] L. N. Trefethen. Pseudospectra of linear operators. *SIAM Rev.*, 39(3):383–406, September 1997.